Supplementary Information

Cohesin-mediated replication fork tethering enables fork slowing and reversal

González-Acosta. Daniel[1, 4, *], Giménez-Llorente. Daniel[2, 4], Rodrigues. Melani[1], Aouami. Moses[1], Barroso-Gomila. Orhi[3], Muñoz. Javier[3], Cuadrado. Ana[2], Losada. Ana[2, *], Lopes. Massimo[1, *]

*Corresponding authors. Email: M.L., lopes@imcr.uzh.ch; D.G.A., gonzalez@imcr.uzh.ch; A:L., alosada@cnio.es

Deleted: , *

List of Supplementary Information:

Materials and Methods

Cell culture

HCT116 cells and derivate cell lines (Extended Data Table 1) were grown in DMEM (Life Technologies, 41966-029) supplemented with 10% fetal bovine serum (FBS, GIBCO), 100 U/ml penicillin and 100 mg/ml streptomycin in an atmosphere containing 6% CO_2 at 37°C. HCT116 OsTIR (F74G), mAID-mClover-RAD21 HCT116 OsTIR (F74G)[1], WAPL-mClover-mAID HCT116 OsTIR (F74G)[2] and CTCF-mClover-mAID HCT116 OsTIR (F74G)[1] were kindly provided by Dr. Masato Kanemaki. To degrade mAID-tagged proteins, cells were treated with 2 µM 5-Ph-IAA (auxin; BioAcademia). To degrade Halo-SMARCAL1, cells were treated with Halo-PROTAC3 at 1:1000 for the indicated times.

Cell line generation

Cell lines were generated following published protocols[3,4]. HCT116 OsTIR (F74G) cells were transfected with CRISPR–Cas9 and donor plasmids using FuGENE HD Transfection Reagent (Promega) in a 12-well plate following the manufacturer's instructions. Two days after transfection, cells were plated in 10 cm^2 dishes and selected with antibiotics. Selected clones were isolated and confirmed for protein expression of the modified alleles. Oligonucleotides to generate sgRNA or amplify homology arms to build donor plasmids are provided in Extended Data Table 1.

RNA interference

For RNA interference cells were transfected with the indicated siRNAs (Extended Data Table 1) for the indicated times and concentration. Transfections were carried out using RNAiMax (Thermo Fisher) according to manufacturer's instruction.

Lentiviral transduction

For cell lines expressing $SMC1^{WT}$, $SMC1^{3D}$ or $SMC1^{4E}$, SMC1-3xFLAG variant genes were cloned into LT3GEPIR (generated by GeneScript) and transfected into to HEK293T cells together with the lentiviral packaging vectors. After 48 h, lentiviral culture medium was harvested, filtered, and added to SMC1-mClover-mAID HCT116 OsTIR (F74G) cells. After infection for 24 h, puromycin (2 µg/ml, InvivoGen) resistant single cells were isolated. To induce the expression of the SMC1 variants cells were treated with 1 µg/mL doxycycline (dox, Sigma-Aldrich).

iPOND-MS

iPOND was performed as described[5,6] with minor modifications. HCT116 cells were labeled with 10 µM EdU for 10 min and treated with the different drugs as indicated in fig. S1A. Cells were crosslinked with 1% formaldehyde for 20 min at room temperature (RT), quenched with 0.125 M glycine for 5 min, and washed three times with cold PBS. EdU was linked to biotin, after permeabilization with 0.25% Triton X-100/PBS for 30 min, by incubating in click reaction buffer (10 mM sodium-L-ascorbate, 20 µM biotin azide (Vanderbilt University), and 2 mM $CuSO_4$) at RT for 1 h on a rotator. Cells were washed twice with PBS, resuspended in lysis buffer (50 mM

Tris-HCl, pH 8.0, and 1% SDS) supplemented with protease inhibitors and chromatin was solubilized by sonication in a Bioruptor Pico (Diagenode) at 4°C 10 min (30 seconds on and 30 seconds off cycles). After centrifugation for 10 min at 16,000 RCF, supernatants were diluted with 1:1 PBS (vol/vol) containing protease inhibitors and incubated overnight with myOne streptavidin C1 dynabeads (Thermo Fisher). Beads were washed once with lysis buffer, once with 1 M NaCl, twice with lysis buffer, and once with PBS. Captured proteins were digested on beads using 500 ng of sequencing grade modified Trypsin (Promega, V5111) including reduction and alkylation of Cysteines with Tris(2-carboxyethyl)phosphine hydrochloride (TCEP) and 2-Chloroacetamide (ClAA) addition, respectively. Resulting peptides were cleaned using the Phoenix kit (Preomics) according to kit instructions. LC-MS/MS analysis of peptide mixture was conducted on an Orbitrap Exploris 480 mass spectrometer (Thermo Fisher) directly coupled to an ACQUITY UPLC M-Class System (Waters) configured for 75-mircom scale single-pump trapping. Peptides were separated on a nanoEase HSS C18 T3, 100A, 75 um x 250 mm analytical column (Waters, PN: 186008818) at a constant flow rate of 300 nl/min applying a peace-wise linear gradient from 5 to 33% solvent B in 45 min (solvent A: water incl. 0.1% formic acid, solvent B: acetonitrile incl. 0.1% formic acid). MS data acquisition was conducted in data-independent mode. DIA scans were acquired in the Orbitrap mass analyzer at 15,000 Resolution (norm. AGC target: 3000%, maxIT: 23 ms) covering the m/z range from 350 to 1050 in 70 non-overlapping isolation windows. Precursors were quadrupole isolated at 10 m/z and HCD fragmented at a NCE of 28 (calculated for middle of isolation window and charge 2).

Data analysis was performed using the PROSTAR package (v1.34.6) in R (v4.3.3). Protein intensity values were log2-transformed and missing values for partially observed values were imputed using the SLSA (Structured Least Squares Algorithm). Data normalization was carried out first within groups and subsequently globally (excluding no biotin and thymidine chase controls) using the LOESS method. The normalized dataset was further processed in Perseus (v1.6.10.50), where remaining missing values were imputed from a normal distribution. For each comparison, proteins were retained only if at least two non-imputed valid values were present in at least one group. The resulting dataset was re-imported into PROSTAR, and differential abundance analysis was performed using the LIMMA test with a log2 fold change (FC) threshold of 0.5. Benjamini-Hochberg correction was used to calculate p-values and FDR. Volcano plots were generated using GraphPad Prism (v10).

PLA and SIRF

Cells were asynchronously grown on poly-lysine coated coverslips. Cells were labeled with 25 μM EdU (Thermo Fisher) for 10 min. After the indicated treatments, cells were washed with PBS and pre-extracted for 5 min using CSK-buffer (10 mM HEPES, 50 mM NaCl, 0.3 M Sucrose, 3 mM $MgCl_2$, 1 mM EDTA or 1 mM EGTA, and 0.5% Triton X-100) at 4ºC, followed by fixation in 4% formaldehyde at RT for 15 min. Upon fixation, cells were washed three times with PBS. In SIRF experiments, EdU was linked to biotin by incubating in click reaction (0.1 M Tris pH 8.5, 0.1 M sodium-L-ascorbate, 2 mM $CuSO_4$ and 0.1 mM biotin-azide) for 1 h at 37 ºC in a humidified chamber. After three washes with PBS, cells were incubated in blocking buffer (5% BSA in PBS) at 37 ºC for 1 h and incubated overnight at 4°C with the indicated antibodies (Extended Data Table 1). After washing twice for 5 min with TBS-T (0.05% Tween-20 in TBS) cells were incubated with PLA probes (Merck) for 1 h at 37 °C, ligation for 30 min at 37 °C, and polymerase reaction for 100 min at 37 °C according to the manufacturer's instructions. After washing twice for 5 min

with TBS, cells were incubated at 37 ºC for 30 min with fluorescently labeled secondary antibodies (Extended Data Table 1), against the individual targets of the PLA, in TBS containing DAPI (0.5 µg/mL). Following two 5-min washes in TBS and letting coverslips air-dry in the dark, coverslips were mounted with Prolong Gold antifade reagent. Microscopy imaging was performed using a Leica DM6 B microscope (HCX PL APO 63x objective). SIRF/PLA and individual channel quantification was performed using Cell Profiler; and plotted and statistically assessed using GraphPad Prism 10. At least 100 cells were measured per condition.

Biochemical fractionation, co-immunoprecipitation assays and WB

Biochemical fractionation of cells was performed as previously described[5,6]. Co-immunoprecipitation experiments were performed by lysing cells in a buffer consisting of 20 mM Tris (pH 7.5), 150 mM NaCl, 5 mM $MgCl_2$, 2 mM NaF, 10% glycerol, 0.2% NP40, 20 mM b-glycerophosphate, 0.5 mM DTT, protease inhibitor cocktail and Benzonase (Millipore), and rotated at 4ºC for 4 h. Lysates were centrifuged at 16000 x g for 30 min at 4°C. Supernatants were incubated with anti-Flag M2 affinity beads (Merck) overnight at 4°C. Beads were washed three times with Lysis buffer. Biochemical fractions, co-immunoprecipitation beads and total cell extracts were prepared in Laemmli sample buffer (4% SDS, 20% glycerol, and 120 mM Tris- HCl, pH 6.8) and loaded onto 4%–20% Mini-PROTEAN TGX Precast Protein Gels (BioRad). For BRCA2 detection, extracts were run in 3 to 8% NuPAGE™ Tris-Acetate Midi Protein Gels (Thermo Fisher). Proteins from all gels were separated by electrophoresis at 180V followed by protein transfer to a nitrocellulose membrane in transfer buffer (25 mM Tris and 192 mM glycine) containing 20% methanol. Before addition of primary antibodies, membranes were blocked in 5% milk in 0.1% TBST (1 × TBS supplemented with 0.1% Tween-20) for 1 h and incubated in 3% BSA with primary antibodies overnight at 4°C (Extended Data Table 1). Secondary antibodies were added for 1 h at RT (in blocking solution; Extended Data Table 1). Membranes were washed three times with 0.1% TBST, 10 min each, after primary and secondary antibody incubations and detected with ECL detection reagent (GE healthcare).

Flow cytometry

Cell lines were labeled with 25 µM EdU for 30 min, harvested by standard trypsinization, washed with PBS once and fixed for 12 min with 4% formaldehyde in PBS. Cells were permeabilized with 0.25% Triton-X in PBS, washed twice with PBS, and EdU was labeled by incubating in click reaction (0.1 M Tris pH 8.5, 0.1 M sodium-L-ascorbate, 2 mM $CuSO_4$ and 0.1 mM Alexa Fluor-linked azide (Thermo Fisher)) for 1 h at RT. Cells were washed twice with PBS and DNA was stained with 1 µg/mL DAPI in PBS for 1 h. Samples were run on Attune NxT Flow Cytometer (Thermo Fisher) and analyzed using FlowJo software V.10.0.8 (FlowJo, LLC). At least 10000 cells were measured per condition.

Metaphase Spreads

Asynchronous mAID-mClover-Sororin cells were treated with 2 µM Aux and/or Nocodazole for a total of 4 hr. Mitotic cells were collected by shake-off, incubated in hypotonic buffer (0.03M sodium citrate), fixed in Carnoy's solution, dropped on acid-washed slides and left overnight at RT. After staining with 1 mg/ml DAPI, slides were mounted with ProLong antifade and left to dry overnight before imaging in a Leica DM6000 microscope with LAS AF software.

Formatted: Font: Italic

DNA fiber assays

All cell lines subjected to this analysis were grown asynchronously and labeled with 30 µM of the thymidine analog 5-Chloro-2'-deoxyuridine (CldU; Sigma-Aldrich) for 30 min, washed three times with warm PBS and exposed to 250 µM of 5-Iodo-2′-deoxyuridine (IdU) for 30 min. For fork progression and S1 DNA fiber assessments IdU was added alone or in combination with the indicated genotoxic treatments and concentrations. For fork degradation assays, IdU was added alone for 30 min, cells were washed three times with PBS and media containing 4 mM HU was added for 3 h. All cells were collected by trypsinization. For S1 assays, cells were incubated with S1 and prepared for spreading as described in[7]. All cells or nuclei were resuspended in cold PBS at 5×10^5 cells/mL or 2×10^6 nuclei/mL. 2 µL of this cell suspension were mixed with 7 µL of lysis buffer (200 mM Tris-HCl, pH 7.5, 50 mM EDTA, and 0.5% SDS) on a glass slide. After an incubation of 6 min at RT, the slides were tilted at a 45° angle to stretch the DNA fibers onto the slide. The resulting DNA spreads were air-dried and fixed in 3:1 methanol/acetic acid. The DNA fibers were denatured by incubating them in 2.5 M HCl for 1 h at RT, washed three times with PBS and blocked with 1% BSA in PBS-T (0.05% Tween-20 in PBS) for 1 h at RT. CldU and IdU tracks were stained for 2 h at RT using two different anti-BrdU antibodies recognizing CldU and, respectively (Extended Data Table 1). After washing three times with PBS, slides were stained with secondary antibodies (Extended Data Table 1) for 1 h at RT in the dark. The slides were mounted in 30 µL Prolong Gold antifade reagent (Invitrogen). Microscopy was done using a Leica DM6 B microscope (HCX PL APO 63x objective). At least 100 fibers per sample were measured using ImageJ. Values were plotted and statistically assessed using GraphPad Prism 10.

Electron microscopy

Cells were asynchronously grown, treated with 1 µg/mL dox for 48 h, 2 µM auxin for 5 h, and 50 µM HU where indicated. Cells were collected, resuspended in ice-cold PBS and crosslinked with 10 µg/mL 4,5′, 8-trimethylpsoralen and pulses of UV 365 nm irradiation with monochromatic light (UV Stratalinker 1800; Agilent Technologies). DNA was extracted as previously described [8]. Briefly, cells were lysed (1.28 M sucrose, 40 mM Tris-HCl [pH 7.5], 20 mM $MgCl_2$, and 4% Triton X-100; Qiagen) and digested (800 mM guanidine-HCl, 30 mM Tris-HCl pH 8.0, 30 mM EDTA pH 8.0, 5% Tween-20, and 0.5% Triton X-100) at 50°C for 2 h in presence of 1 mg/mL proteinase K. The DNA was purified using chloroform/isoamylalcohol (24:1) and precipitated in one volume of isopropanol. DNA was washed with 70% EtOH and resuspended in 200 µL TE (Tris-EDTA) buffer. 6 µg of DNA were incubated with 120 U of PvuII HF (New England Biolabs) for 5 h at 37ºC. RNase A (Sigma–Aldrich, R5503) was added to a final concentration of 250 µg/ml for the last 2 h of this incubation. Digested DNA was purified using a Silica Bead Gel Extraction kit (Thermo Fisher Scientific) according to manufacturer's instructions. DNA was spread on a carbon-coated 400-mesh nickel grids (G2400N, Plano Gmbh using Benzyl-dimethyl-alkyl-ammonium chloride (BAC). DNA was then coated with platinum using a High Vacuum Evaporator (EM BAF060, Leica) as previously described[8]. The grids were imaged automatically at 28'000x using a Talos 120 transmission electron microscope (FEI; LaB6 filament, high tension ≤120 kV) with a bottom-mounted CMOS camera BM-Ceta (4096x4096 pixels) and the MAPS 3 software (Thermo Fisher Scientific). For analysis, samples were annotated for replication intermediates using the MAPS offline viewer (V3.28, Thermo Fisher Scientific) and corresponding images were extracted. The replication intermediates were scored blind to the experimental

condition using Fiji[9]. For each experimental condition at least 65 replication fork molecules were analyzed in two distinct biological replicates. Values were plotted and statistically assessed using GraphPad Prism 10.

Proliferation and clonogenic assay

Cells were treated with 1 µg/mL of dox for 48 h (for WT and 4E-SMC1 substituted cells) and 2 µM auxin (1 d before treatment in NIPBL degron cells, and 3 d before treatment in SMC1-substituted cells). 1000 cells were seeded in each well of a 6-well plate. Cells were then optionally treated with 90 nM MMC (Sigma-Aldrich) for 24h, washed, and incubated in normal media, or treated with 150 µM HU (Sigma-Aldrich) or 50 nM Aph (Sigma-Aldrich) for 9 d to allow formation of colonies. Subsequently, colonies were stained with 0.5% (w/v) crystal violet in 20% ethanol. Plates were imaged using a plate reader and the number of colonies were quantified using ImageJ. Values were normalized to the UNT control, and then plotted and statistically assessed using GraphPad Prism 10.

Micro-C experiments

The Micro-C library was prepared using the Dovetail® Micro-C Kit according to the manufacturer's protocol. Briefly, cells were treated with 1 µg/mL dox for 48 h, 2 µM auxin for 5 h where indicated. The chromatin was fixed with disuccinimidyl glutarate (DSG) and formaldehyde in the nucleus. The cross-linked chromatin was then digested in situ with micrococcal nuclease (MNase). Following digestion, the cells were lysed with SDS to extract the chromatin fragments and the chromatin fragments were bound to Chromatin Capture Beads. Next, the chromatin ends were repaired and ligated to a biotinylated bridge adapter followed by proximity ligation of adapter-containing ends. After proximity ligation, the crosslinks were reversed, the associated proteins were degraded, and the DNA was purified and then converted into a sequencing library using Illumina-compatible adaptors. Biotin-containing fragments were isolated using streptavidin beads prior to PCR amplification.

Repli-C experiments

Cells were treated with 1 µg/mL dox for 48h, 2 µ M auxin for 5 h where indicated. 10 µM EdU was added for 15 min, either before collection or before washing and treating cells with 2 mM HU for 2 h. Repli-C was performed using the Dovetail® HiChIP MNase Kit with modifications. Cells were collected by trypsinization, the chromatin was fixed with DSG and formaldehyde, and permeabilized with 0.25% Triton-X in PBS. EdU was clicked to digoxigenin by incubating in click reaction (0.1 M Tris pH 8.5, 0.1 M sodium-L-ascorbate, 2 mM $CuSO_4$ and 0.3 mM digoxigenin-azide (ATTBio)). After, cross-linked chromatin was digested in situ with MNase then extracted upon cell lysis using a combination of RIPA lysis and gentle sonication using Bioruptor Pico in RIPA buffer. The chromatin fragments were incubated with anti-digoxigenin antibody pre-coupled to A/G-coated beads, overnight rotating at 4ºC. Next, the chromatin ends were repaired and ligated to a biotinylated bridge adapter followed by proximity ligation of adapter-containing ends. After proximity ligation, the crosslinks were reversed, the associated proteins were degraded, and the DNA was purified then converted into a sequencing library using Illumina-compatible adaptors. Biotin-containing fragments were isolated using streptavidin beads prior to PCR amplification.

Micro-C and Repli-C analyses

Micro-C/Repli-C data were processed using a standardized Hi-C analysis pipeline. Raw paired-end sequencing reads were quality-trimmed using Trim Galore (quality threshold = 20, minimum length = 30 bp) and aligned to the hg38 human reference genome using BWA-MEM[10]) with Hi-C-specific parameters (-5SP -T0). Aligned reads were processed with the pairtools suite: contacts were parsed with a minimum mapping quality of 40 (--min-mapq 40), allowing walks of up to 5 unique alignments (--walks-policy 5unique) with a maximum inter-alignment gap of 30 bp. Parsed pairs were sorted, and PCR duplicates were removed while retaining duplicate marking statistics. Valid contact pairs were converted to ".hic" format using Juicer Tools (v1.22.01) and to multi-resolution cool format (.mcool) using HiCExplorer with Knight-Ruiz (KR) matrix balancing normalization. For comparative analyses between conditions, biological replicates were merged using pairtools merge, and datasets were downsampled to equalize sequencing depth across conditions using pairtools sample. Downsampling fractions were calculated to match the condition with the lowest sequencing depth, ensuring unbiased comparisons (Extended Data Table 2). Contact probability as a function of genomic distance was calculated as an intra-chromosomal contact frequency distribution, using logarithmically increasing genomic distance bins. The insulation score was computed using a custom Python script following the methodology described in[11], extracting 10-kb resolution raw matrices and using a sliding window of 100 kb x 100 kb. Chromatin loops were detected using Chromosight[12] on balanced contact matrices at 25 kb resolution, with a scanning distance range of 50 kb to 1 Mb. Additionally, architectural stripes (left and right patterns) were identified at 25 kb resolution.

Replication fountains, characterized by enriched long-range chromatin interactions radiating from replication origins, were identified using the FUN (Fountains Using Neighborhoods) algorithm[13] on balanced contact matrices at 10 kb and 25 kb resolutions. Signal-over-Noise (SoN) scores were calculated using a sliding window approach with an extension length of 500 kb, offset of 50 kb, and padding widths of 3 bins (10 kb) or 1 bin (25 kb). Fountain structures were detected by extending outward from SoN summits (extension pixels: 6-100 bins, step size 2 at 10 kb; 3-35 bins, step size 1 at 25 kb) and evaluated for statistical significance (p-value < 0.05, signal-to-background ratio > 1.3).

Metaplots were created using coolpuppy[14] on Knight-Ruiz balanced matrices. In the Inter-replication fork metaplots, the –scale option was added to scale all the regions to the same size. Intra-replicon was quantified from metaplot diagonal decay profiles by calculating the log2 fold-change ratio between short-range (≤50 kb) and mid-range (50-100 kb) normalized contact frequencies. For each condition, diagonal decay was computed by extracting contact values at increasing distances from the diagonal using a sliding window approach (3 bins each side of the center point), with background normalization calculated from an extended window (10 bins). Values were log2-transformed and smoothed using a 3-point moving average kernel. The intra-replicon contact index was defined as log2(mean contacts ≤50kb / mean contacts 50-100kb), where higher values indicate increased short-range contacts. Values were plotted and statistically assessed using GraphPad Prism 10. Inter-replication fork interaction strength was quantified by extracting the sum of log2 contact frequencies from a 6×6 pixel region centered in the origin-origin interaction, representing the enrichment of contacts between paired replication origins.

Identification of replication origins

Replication Fork Directionality (RFD) profiles were obtained from published Pu-seq data[15], which quantifies the differential usage of leading and lagging strand DNA polymerases during replication. To identify replication origins, we analyzed the RFD signal across the genome at 10-kb resolution. For each chromosome (excluding chrM and chrY), binned mean values were extracted and smoothed using a moving average filter (window size = 5) followed by Savitzky-Golay filtering (window = 15, polynomial order = 3) to preserve signal features while reducing noise. Replication origins and termination zones were identified by detecting inflection points in the smoothed RFD profile through second derivative analysis. The second derivative captures the curvature of the signal, identifying the precise genomic positions where replication fork dynamics fundamentally change. Replication origins were called as downward inflection points (second derivative changes from positive to negative), corresponding to bidirectional fork movement away from the origin. For each putative origin, replication strength was calculated as the difference between the maximum RFD value in the downstream region (between the origin and the next termination zone) and the minimum RFD value in the upstream region (between the previous termination zone and the origin). Origins with replication strength below a threshold of 0.05 were considered weak and excluded from further analysis. When weak origins were removed, adjacent termination zones were merged by averaging their genomic positions. The remaining strong origins were reassigned to their flanking termination zones to ensure consistency between origin and termination zone annotations. Origins lacking flanking termination zones on either side were discarded.

Statistical analyses and graph representation

For SIRF, PLA, DNA fiber and Chromatin bound RAD21 immunofluorescence, individual dots represent values for one of the triplicates with the horizontal black bar being the median of the values for that replicate. Error bars and orange dots represent the median values of the three replicates. Exact p-values for the indicated comparisons are provided. Statistical assessment was performed on the three median values. When the experiment contained only two conditions, t-test followed by Bonferroni post-test was applied. For experiments with more than two conditions, one-way ANOVA followed by Bonferroni post-test was applied.

For clonogenic assays, cell proliferation or SMC1 immunofluorescence, exact p-values for the indicated comparisons are provided. Statistical assessment was performed on the three median values. One-way ANOVA followed by Bonferroni post-test was applied.

For loop length assessment, individual values with exact p-values for the indicated comparisons are provided. When the experiment contained only two conditions, non-parametric t-test followed by Mann-Whitney post-test was applied. For experiments with more than two, non-parametric one-way ANOVA followed by Kruskal-Wallis post-test was applied.

Extended Data Figure 1.

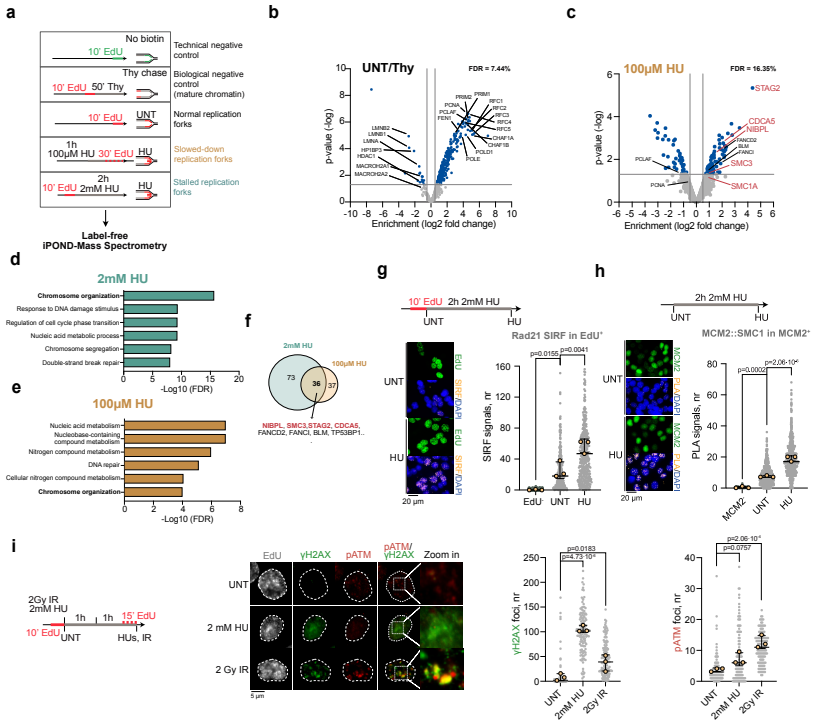

Extended Data Fig. 1. iPOND-MS analyses under fork slowing and stalling conditions with PLA validations. (**a**). Experimental conditions included in the iPOND-MS experiment. (**b**). Volcano plot of iPOND-MS data showing enrichment (log2 fold change) and significance (-log p-value) of the different proteins in untreated control compared to the Thy chase condition. Selected protein hits are indicated to highlight enrichment of replisome components in the untreated control, and enrichment of mature chromatin proteins in the Thy chase condition. FDR for the selected comparison at p-value 0.05 is shown. (**c**). Volcano plot of iPOND-MS data showing enrichment (log2 fold change) and significance (-log p-value) of the different proteins in untreated control compared to the 100 μM HU condition. Selected protein hits are indicated to highlight enrichment 100 μM HU over the untreated control. Cohesin subunits are shown in red. FDR for the selected comparison at p-value 0.05 is shown. (**d** and **e**). PANTHER Gene Ontology (GO) analyses of biological pathways in iPOND-MS hits of 2 mM HU and 100 μM HU, respectively. Significance is assessed with -Log10 of False Discovery Rate (FDR). (**f**). Venn diagram showing number of specific and overlapped protein hits found enriched in 2 mM HU and 100 μM HU conditions. Examples of protein hits found enriched in both are shown. (**g**). RAD21 SIRF upon 2 mM HU. EdU^{-} cells from the UNT condition are shown as a control. (**h**). MCM2::SMC1 PLA upon 2 mM HU. MCM2^{-} cells (G2 cells lacking MCM2 staining) from the UNT condition serve as a negative control. (**i**). γH2AX and pATM immunofluorescence staining and quantifications of cells treated with 2mM HU or 2Gy γ-irradiation.

Deleted: are shown

Deleted: ¶

Extended Data Figure 2.

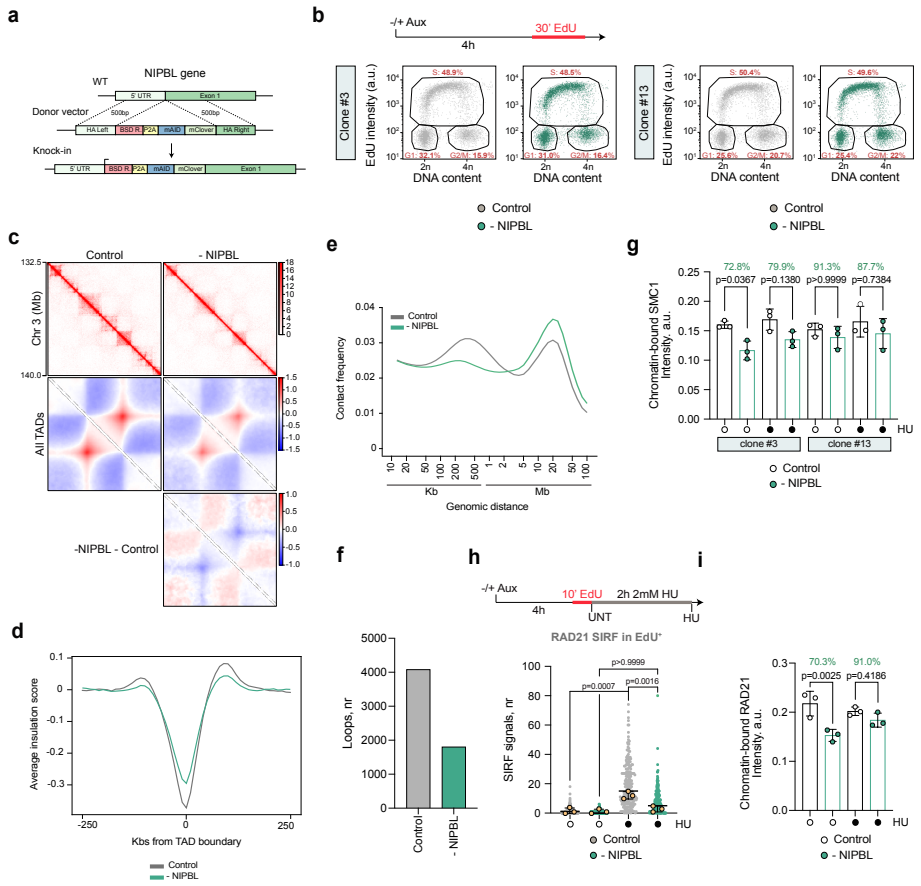

Extended Data Fig. 2. Characterization of DNA replication and genome organization after NIPBL depletion in mAID-mClover-NIPBL HCT116 cells. (**a**). Schematic of mAID-mClover cassette insertion into the start codon of the *NIPBL* gene. (**b**). EdU versus DAPI intensity flow cytometry profiles, after incorporation of EdU for 30 min. (**c**). Micro-C contact matrices from the indicated region. Below, aggregate analysis of chromatin contacts at re-scaled TADs. Differential enrichment of signals from aggregated analyses of -NIPBL minus Control. (**d**). Average insulation score around TAD boundaries. (**e**). Contact frequency distribution plotted as a function of genomic distance in the absence of NIPBL. (**f**). Quantification of the number of loops. (**g**). SMC1 intensity on chromatin after NIPBL depletion from the same cells as Fig. 1f. (**h**). RAD21 SIRF upon 2 mM HU in NIPBL-degron cells. (**i**). RAD21 intensity on chromatin after NIPBL depletion from the same cells as in (H).

Deleted: TADs are re-scaled to the same length. (**d**).

Deleted: (c)

Deleted: e

Moved (insertion) [1]

Deleted: f

Moved up [1]: Contact frequency distribution plotted as a function of genomic distance. In the absence of NIPBL

Deleted: . I

Deleted: Quantification of the number of loops.

Deleted: g

Deleted: .

Deleted: , contacts in the cohesin-mediated loop range decrease while very long contacts, corresponding to compartments, increase

Deleted: h

Formatted: Font: Bold

Formatted: Font: Bold

Extended Data Figure 3.

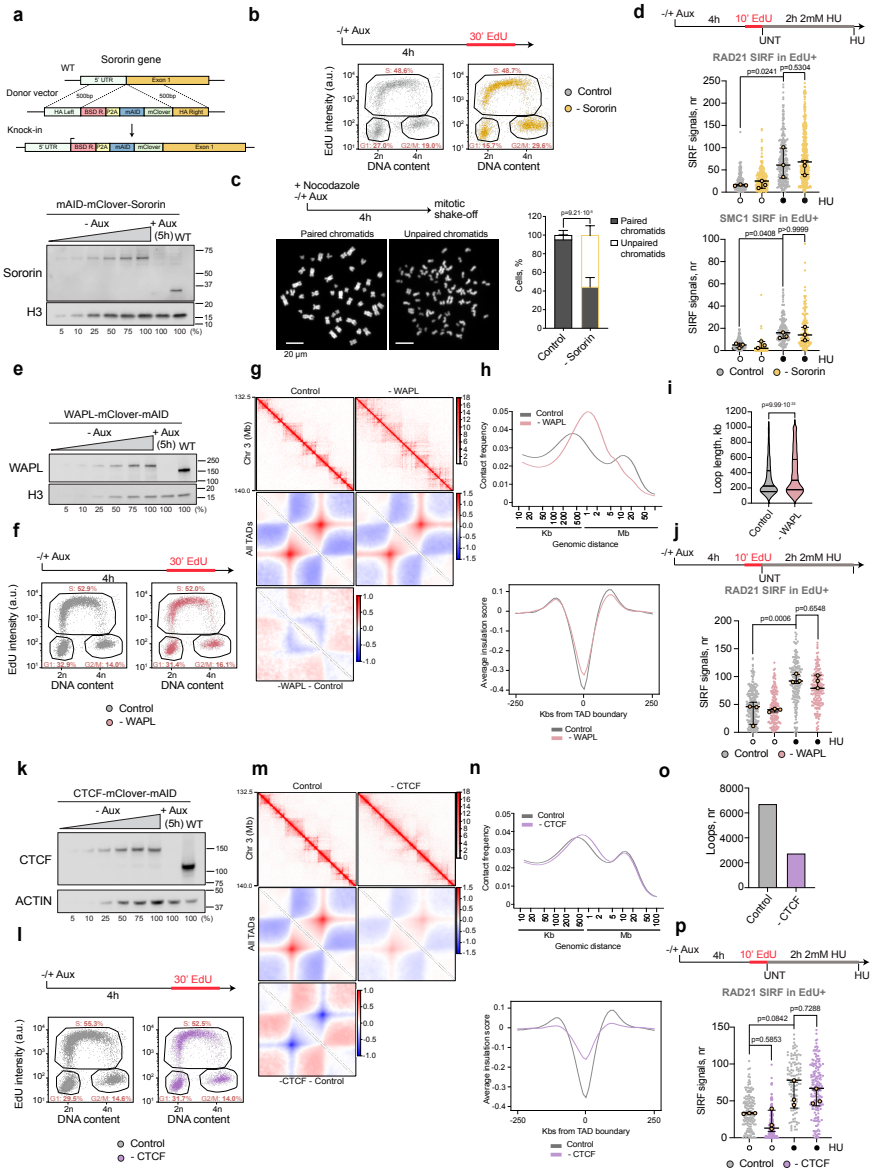

Extended Data Fig. 3. Effect of Sororin, WAPL or CTCF depletion on cohesin accumulation at stalled forks. (**a**). Schematic of mAID-mClover cassette insertion into the start codon of the *Sororin (CDCA5)* gene. Below, immunoblot of Sororin and H3 (loading control) in mAID-mClover-Sororin. (**b**). EdU versus DAPI intensity flow cytometry profiles, after incorporation of EdU for 30 min. (**c**). Metaphase spreads after 4h of Nocodazole and Aux treatments in Sororin-degron cells. (**d**). RAD21 and SMC1 SIRFs upon 2 mM HU in the indicated conditions. (**e**). Immunoblot of WAPL and H3 (loading control) in WAPL-mClover-mAID cells. (**f**). EdU versus DAPI intensity flow cytometry profiles, after incorporation of EdU for 30 min. (**g**). Micro-C contact matrices from the indicated region. Below, aggregate analysis of chromatin contacts at re-scaled TADs. Differential enrichment of signals from aggregated analyses of -WAPL minus Control. (**h**). Average insulation score around TAD boundaries and contact frequency distribution plotted as a function of genomic distance in the absence of WAPL. (**i**). Quantification of loop length. (**j**). RAD21 SIRF upon 2 mM HU in the indicated conditions. (**k**). Immunoblot of CTCF and ACTIN (loading control) in CTCF-mClover-mAID cells. (**l**). EdU versus DAPI intensity flow cytometry profiles, after incorporation of EdU for 30 min. (**m**). Micro-C contact matrices from the indicated region. Below, aggregate analysis of chromatin contacts at re-scaled TADs. Differential enrichment of signals from aggregated analyses of -CTCF minus Control. (**n**). Average insulation score around TAD boundaries and contact frequency distribution plotted as a function of genomic distance in the absence of CTCF. (**o**). Quantification of the number of loops. (**p**). RAD21 SIRF upon 2 mM HU treatment in the indicated conditions.

Deleted: d
Formatted: Font: Bold
Deleted: e
Deleted: f
Formatted: Font: Bold
Formatted: Font: Bold
Deleted: g
Formatted: Font: Bold
Deleted: h
Deleted: i

Extended Data Figure 4.

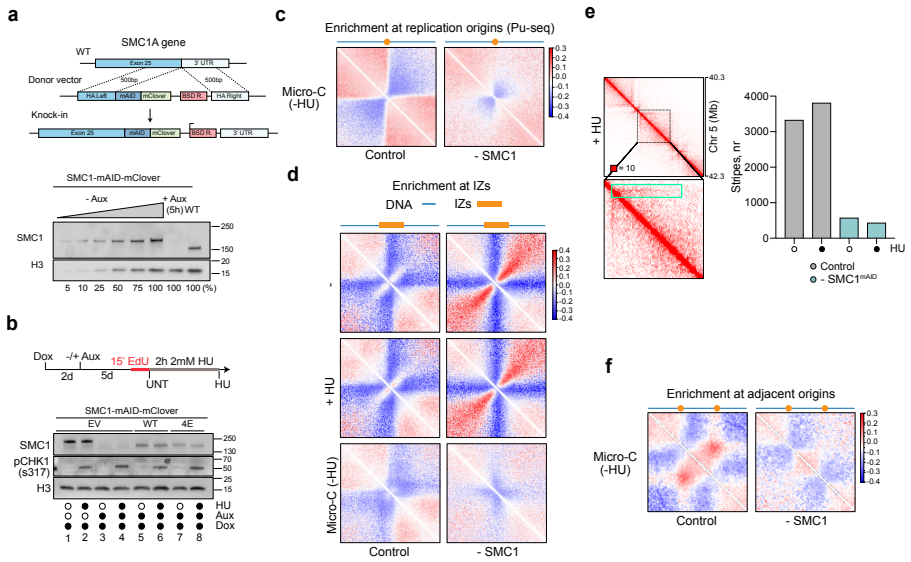

Extended Data Fig. 4. Analyses of Repli-C data upon RS and SMC1 depletion. (**a**). Schematic of mAID-mClover cassette insertion into the stop codon of the *SMC1A* gene. Immunoblot of SMC1 and H3 (loading control) in SMC1-mClover-mAID. (**b**). Experimental set up and immunoblot of SMC1, phospho-CHK1 (Ser317) and H3 (loading control) in SMC1-mClover-mAID cells. (**c**). Aggregated analysis of Micro-C contacts around replication origins (Pu-seq). (**d**). Aggregated analysis of Repli-C and Micro-C contacts around IZs. (**e**). Quantification of the number of stripes at the indicated conditions. (**f**). Aggregate analysis of Micro-C contacts at regions with adjacent origins (200-400 kb separation).

Extended Data Figure 5.

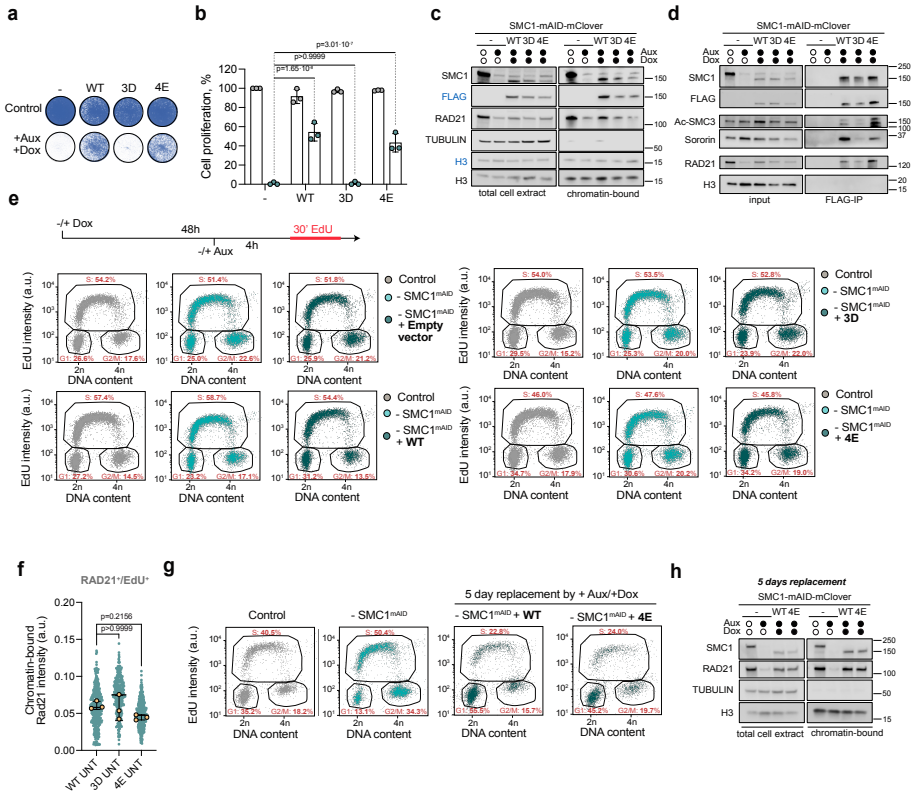

Extended Data Fig. 5. Characterization of cohesin mutants' protein interactions and replication dynamics. (**a**). Representative images of cell proliferation staining. (**b**). Quantification of cell proliferation in the indicated SMC1-FLAG substituted conditions. (**c**). Immunoblot of SMC1, FLAG, RAD21, TUBULIN (fractionation control) and H3 (loading control) in total cell extract and chromatin-bound fraction. Blue labels correspond to a separate WB run. (**d**). Immunoblot of SMC1, FLAG, Acetylated-SMC3, Sororin, RAD21 and H3 (immunoprecipitation control) after FLAG immunoprecipitation (IP). (**e** and **g**). EdU versus DAPI intensity flow cytometry profiles, after incorporation of EdU for 30 min. (**f**). Chromatin-bound RAD21 intensity in the experiment from Fig. 2j. (**h**). Immunoblot of SMC1, RAD21, Tubulin (fractionation control) and H3 (loading control) in total cell extract and chromatin-bound fraction.

Deleted: f

Formatted: Font: Bold

Deleted: g

Extended Data Figure 6

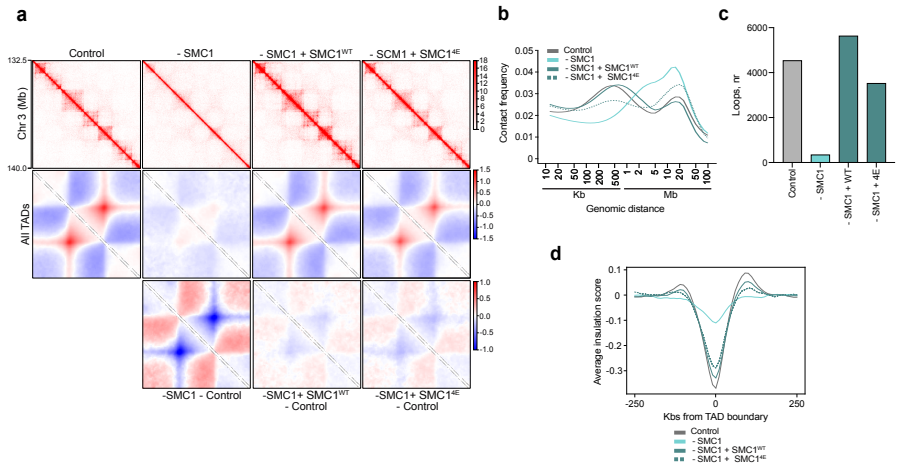

Extended Data Fig. 6. Analyses of genome organization of SMC1^{4E}-substituted cells. (**a**). Micro-C contact matrices from the indicated region. Middle row, aggregate analysis of chromatin contacts at TADs. TADs are re-scaled to the same length. Bottom row, differential enrichment of signals from aggregated analyses of -SMC1, SMC1^{WT} or SMC1^{4E} minus Control. (**b**). Contact frequency distribution plotted as a function of genomic distance. (**c**). Quantification of the number of loops. (**d**). Average insulation score around TAD boundaries.

Extended Data Figure 7

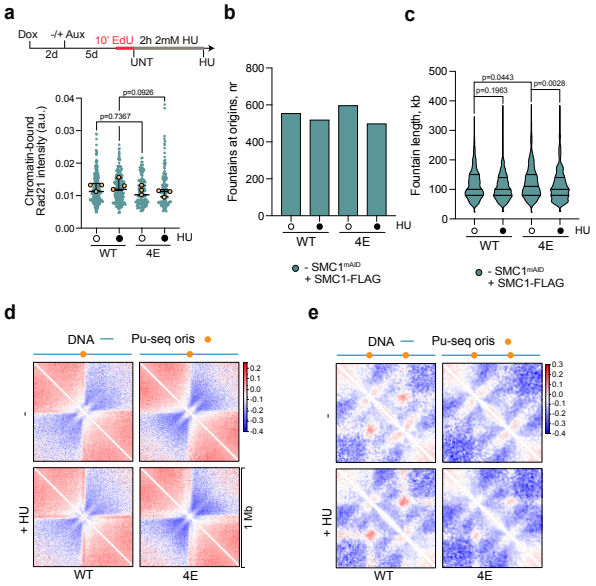

Extended Data Fig. 7. Chromatin binding of SMC1^{4E} and Repli-C analyses of SMC1^{4E}-substituted cells upon RS. (**a**). Chromatin-bound RAD21 intensity in the experiment from Fig. 2K. (**b** and **c**). Number and length of fountains identified at origin positions in the indicated conditions. (**d**). Aggregated analysis of Repli-C contacts around centered origins (1 Mb). (**e**). Aggregate analysis of Repli-C contacts at regions with adjacent origins (200-400 kb separation).

Extended Data Figure 8

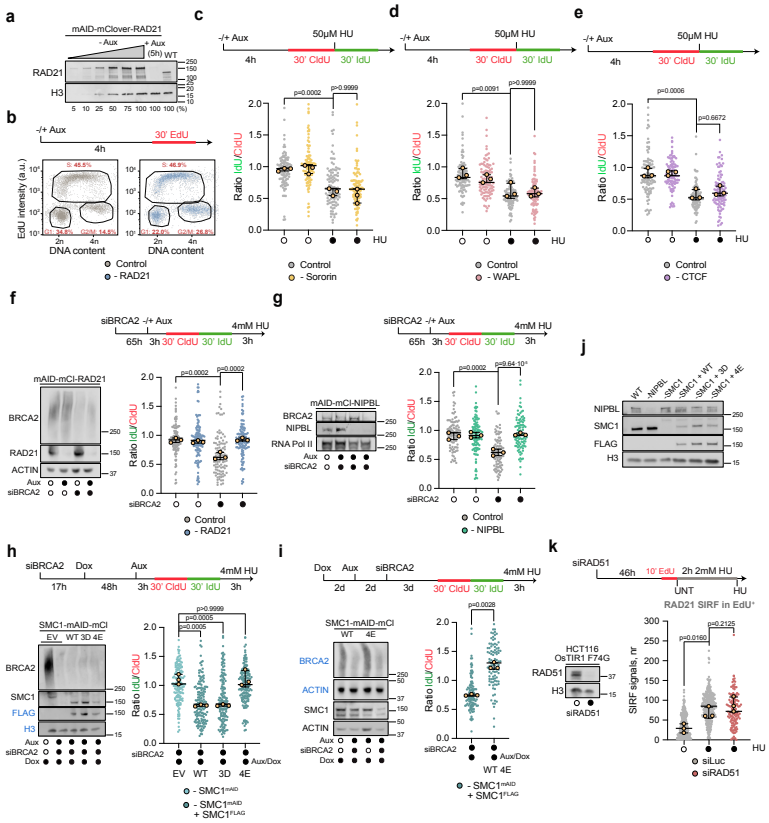

Extended Data Fig. 8. Regulation of fork progression and reversal upon RS by factors involved in genome organization, cohesin and cohesin cofactors. (**a**). Immunoblot of RAD21 and H3 (loading control) in mAID-mClover-RAD21 cells. (**b**). EdU versus DAPI intensity flow cytometry profiles, after incorporation of EdU for 30 min. (**c-e**). IdU/CldU DNA fiber values (upon 50 μM HU) in Sororin, WAPL and CTCF degron cells. (**f**). Immunoblot of BRCA2, RAD21 and ACTIN (loading control). Right, IdU/CldU DNA fiber values (upon 4 mM HU, siBRCA2) in Rad 21 degron cells. (**g**). Immunoblot of BRCA2, NIPBL and RNA Pol II (loading control). Right, IdU/CldU DNA fiber values (upon 4 mM HU, siBRCA2) in NIPBL degron cells. (**h**). Immunoblot of BRCA2, SMC1, FLAG and H3 (loading control). Blue labels correspond to a separate WB run. Right, IdU/CldU DNA fiber values (upon 4 mM HU, siBRCA2) in SMC1 degron cells and its substitution with $SMC1^{WT}$, $SMC1^{3D}$ or $SMC1^{4E}$. (**i**). Immunoblot of BRCA2, SMC1, and ACTIN (loading control). Blue labels correspond to a separate WB run. Right, IdU/CldU DNA fiber values (upon 4 mM HU, siBRCA2) in SMC1 degron cells and its substitution with $SMC1^{WT}$, $SMC1^{4E}$ (5 d). (**j**). Immunoblot of NIPBL, SMC1, FLAG and H3 (loading control). (**k**). Immunoblot of RAD51 and H3 (loading control). RAD21 SIRF upon 2 mM HU in the indicated conditions.

Extended Data Figure 9

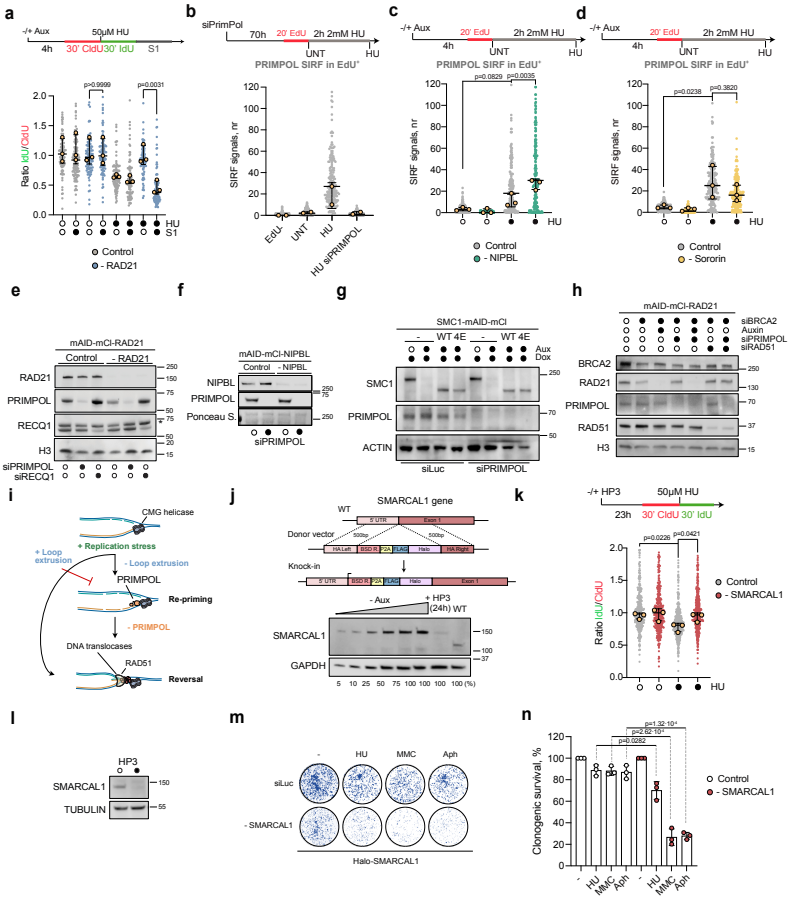

Extended Data Fig. 9. Fork degradation experiments in cohesin separation-of-function mutants. (a). IdU/CldU DNA fiber values in RAD21 degron cells, for the indicated conditions. (**b**). PRIMPOL SIRF upon 2 mM HU in siPrimPol, in NIPBL-degron (**c**) and Sororin-degron (**d**) cells. (**e**). Immunoblot of RAD21, PRIMPOL, RECQ1 and H3 (loading control). (**f**). Immunoblot of NIPBL and PRIMPOL, and Ponceau staining (loading control). (**g**). Immunoblot of SMC1, PRIMPOL, and ACTIN (loading control). (**h**). Immunoblot of BRCA2, RAD21, PRIMPOL, RAD51 and H3 (loading control). (**i**). Role of loop-extruding cohesin in fork plasticity (see text for details). (**j**). Schematic of FLAG-Halo cassette insertion into the start codon of the *SMARCAL1* gene. Below, immunoblot of SMARCAL1 and GAPDH (loading control) in FLAG-Halo-SMARCAL1. (**k**). IdU/CldU DNA fiber values (upon 50 μM HU) in SMARCAL1-degron cells. (**l**). Immunoblot of SMARCAL1 and TUBULIN (loading control) in FLAG-Halo-SMARCAL1 from (M). (**m**). Clonogenic assays in SMARCAL1 degron cells exposed to HU, Aph or MMC as in Fig. 4f and g. (**n**). Quantifications from (M).

Formatted: SM Text, Justified
Formatted: Font: Bold
Formatted: Font: Bold
Deleted: c
Formatted: Font: Bold
Deleted: d
Deleted: e
Deleted: f
Formatted: Font: Bold
Formatted: Font: Bold
Formatted: Font: Bold
Formatted: Font: Bold
Deleted: ¶
Formatted: Font: Bold

Extended Data Table 1

Cell lines		
Reagent	**Source**	**Identifier/Reference**
HCT116	ATCC	CCL-247
HCT116 OsTIR (F74G)	Kanemaki Lab	(*53*, *55*)
mAID-mClover-RAD21 HCT116 OsTIR (F74G)	Kanemaki Lab	(*53*)
WAPL-mClover-mAID HCT116 OsTIR (F74G)	Kanemaki Lab	(*54*)
CTCF-mClover-mAID HCT116 OsTIR (F74G)	Kanemaki Lab	(*53*)
mAID-mClover-NIBPL HCT116 OsTIR (F74G)	This study	This study
mAID-mClover-Sororin HCT116 OsTIR (F74G)	This study	This study
SMC1-mClover-mAID HCT116 OsTIR (F74G)	This study	This study
SMC1-mClover-mAID HCT116 OsTIR (F74G) + $SMC1^{WT}$-3xFLAG	This study	This study
SMC1-mClover-mAID HCT116 OsTIR (F74G) + $SMC1^{3D}$-3xFLAG	This study	This study
SMC1-mClover-mAID HCT116 OsTIR (F74G) + $SMC1^{4E}$-3xFLAG	This study	This study
FLAG-Halo-SMARCAL1 HCT116 OsTIR (F74G)	This study	This study
Oligonucleotide		
Reagent	**Sequence (5'-3')**	**Use**
NIBPL_sgRNA_Fw	CACCGCAACACCATTCCAGAAATTC	NIPBL CRISPR plasmid
NIBPL_sgRNA_Rev	AAACGAATTTCTGGAATGGTGTTGC	NIPBL CRISPR plasmid
NIBPL_HA_Fw	GCTAGAAAGGCAAGTTGAAGCTAGATT	NIPBL donor plasmid
NIBPL_HA_Rev	CAGGTAGGATGACACAGTAACTAAAATTGTAGG	NIPBL donor plasmid
NIBPL_invPCR_Fw	GGATCCAATGGGGATATGCCCCATGTC	NIPBL donor plasmid
NIBPL_invPCR_Rev	GTCGACTCTGAATTTCTGGAATGGTGTTGCC	NIPBL donor plasmid
Sororin_sgRNA_Fw	CACCGTCGCCTCCCAGACATAACTT	Sororin CRISPR plasmid
Sororin_sgRNA_Rev	AAACAAGTTATGTCTGGGAGGCGAC	Sororin CRISPR plasmid
Sororin_HA_Fw	GAGGCTCCCCGATACTACCG	Sororin donor plasmid
Sororin_HA_Rev	CACCCACAACACTCTCCTTAGCC	Sororin donor plasmid

Formatted Table

Sororin_invPCR_Fw	GTCGACCTCCGTCTCGAGCTCCTCCA	Sororin donor plasmid
Sororin_invPCR_Rev	GGATCCTCTGGGAGGCGAACGCG	Sororin donor plasmid
SMC1_sgRNA_Fw	CACCGGCTTAGGGATCCAGACAGGGC	SMC1 CRISPR plasmid
SMC1_sgRNA_Rev	AAACGCCCTGTCTGGATCCCTAAGC	SMC1 CRISPR plasmid
SMC1_HA_Fw	CCTGTCTGGATCCCTAAGCTGT	SMC1 donor plasmid
SMC1_HA_Rev	AAGACTCCTATGAGGTCCTGAGTACC	SMC1 donor plasmid
SMC1_invPCR_Fw	AACCCCAATGAGCAGGGATCCGGTGCAGGCG	SMC1 donor plasmid
SMC1_invPCR_Rev	AGGGATCCAGACAGGGGATCCtAGTGAACCTCTTCGAGG	SMC1 donor plasmid
SMARCAL1_sgRNA_Fw	CACCGAATGTCCTTGCCTCTTACAG	SMARCAL1 CRISPR plasmid
SMARCAL1_sgRNA_Rev	AAACCTGTAAGAGGCAAGGACATTC	SMARCAL1 CRISPR plasmid
SMARCAL1_HA_Fw	TTTGAGAGTTTTGTTCTTGTTGCCC	SMARCAL1 donor plasmid
SMARCAL1_HA_Rev	TTTCACAGAGAAATGCTTATGCAGGAATG	SMARCAL1 donor plasmid
SMARCAL1_invPCR_Fw	AGTCTTCCTCTTACAGAGGAGCAGAGGAAAAAG	SMARCAL1 donor plasmid
SMARCAL1_invPCR_Rev	AGAGGCTTATGAGTTGGGTTAGC	SMARCAL1 donor plasmid
RNAi		
Reagent	**Sequence (5'-3')**	**Concentration and time**
siLuc	CGUACGCGGAAUACUUCGATT	100 nM; 48-72h
siPRIMPOL	GAGGAAACCGUUGUCCUCAGUGUAU	40 nM; 48-72h
siRECQ1	UUACCAGUUACCAGCAUUATT	40 nM; 48h
siBRCA2	UUGACUGAGGCUUGCUCAGUUTT	100 nM; 72h
siRAD51	GACUGCCAGGAUAAAGCUUTT	40 nM; 48-72h
Antibody		
Target	**Source, Identifier**	**Technique (concentration)**
SMC1 #1 (Rb)	Losada Lab, [16]	WB (1:1000), IF/PLA (1:200)
SMC1 #2 (Rb)	Thermo Fisher, PA5-29122	WB (1:1000)
NIPBL (Rb)	Losada Lab, [16]	WB (1:500), IF/PLA (1:200)
RAD21 (Rb)	Abcam, ab217678	WB (1:1000), IF/PLA (1:200)
Sororin (Rb)	Losada Lab, [17]	WB (1:1000)
WAPL (Rb)	Cell Signaling, 77428	WB (1:1000)
CTCF (Rb)	Cell Signaling, 3418	WB (1:1000)
Ac-SMC3 (Ms)	Merck, MABE1925	WB (1:1000)
RNA Pol II RPB1 (Ms)	BioLegend, 920204	WB (1:1000)
H3 (Rb)	Abcam, ab1791	WB (1:10000)

Formatted: Font: (Default) Times New Roman, 9 pt, Font colour: Auto, English (US)

Formatted: Font: (Default) Times New Roman, 9 pt, Font colour: Auto, English (US)

Formatted: Font: (Default) Times New Roman, 9 pt, Font colour: Auto, English (US)

Formatted: Font: (Default) Times New Roman, 9 pt, Font colour: Auto, English (US)

Formatted: Font: (Default) Times New Roman, 9 pt, Font colour: Auto, English (US)

Formatted: Font: (Default) Times New Roman, 9 pt, Font colour: Auto, English (US)

ACTIN (Ms)	Sigma-Aldrich, A2228	WB (1:5000)
FLAG (Ms)	Merck, F3165	WB (1:2000)
PRIMPOL (Rat)	Méndez Lab [18]	WB (Whole serum)
MCM2 (Ms)	Thermo Fisher, MA5-15923	IF/PLA (1:500)
RECQ1 (Rb)	Abcam, ab172607	WB (1:1000)
RAD51 (Rb)	BioAcademia, 70-002	WB (1:1000)
BRCA2 (Ms)	Sigma-Aldrich, OP95	WB (1:1000)
Tubulin (Ms)	Sigma-Aldrich, T6199	WB (1:10000)
SMARCAL1 (Rb)	Abcam, ab154226	WB (1:1000)
GAPDH (Ms)	Sigma-Aldrich, MAB374	WB (1:5000)
phospho-H2AX (Ser 139) (Rb)	Cell Signaling, 9718	IF (1:100)
phospho-ATM (Ser 1981) (Ms)	Thermo Fisher, 200-301-400	IF (1:1000)
phospho-Chk1 (Ser 317) (Rb)	Cell Signaling, 12302	WB (1:1000)
Biotin (Ms)	Jackson ImmunoResearch, 200-002-211	IF/PLA (1:200)
Digoxigenin (Ms)	MBL, M227-3	Repli-C (coupled to beads)
BrdU (CldU; Rat)	Abcam, ab6326	IF (1:150)
BrdU (IdU; Ms)	Becton Dickinson, 347580	IF (1:100)
Alexa 488 (Ms IgG1)	Invitrogen, A-21121	IF (1:300)
Alexa 555 (Rat)	Invitrogen, A-21434	IF (1:300)
Alexa 488 (Ms)	Invitrogen, A-11001	IF (1:500)
Alexa 488 (Rb)	Invitrogen, A-11034	IF (1:500)
Alexa 555 (Ms)	Invitrogen, A-21422	IF (1:500)
Alexa 555 (Rb)	Invitrogen, A-21428	IF (1:500)
Alexa 647 (Ms)	Invitrogen, A-31571	IF (1:500)
F(ab')2 Alexa 647 (Rb)	Invitrogen, A-21246	IF (1:500)
ECL IgG, HRP-linked (Ms)	Sigma-Aldrich, NA934	WB (1:5000)
ECL IgG, HRP-linked (Rb)	Sigma-Aldrich, GENA931	WB (1:5000)
IgG, Cross-Adsorbed, HRP (Rat)	Thermo Fisher, A10549	WB (1:5000)
Publicly available data		
Description	**Source**	**Identifier; Password for reviewers**
iPOND-MS	This study	PXD071150; 1m0QZky7bpkD
Micro-C and Repli-C	This study	GSE311634: ybwhgowmbxotfqb GSE311782: ozkvyeewznajjif
Pu-seq origins and termination zones	[15]	GSE189668
HR Repli-seq initiation zones	[2]	https://data.4dnucleome.org/experiment-sets/4DNESNGZM5FG/
TADs	[19]	GSE104334
Cohesin and CTCF ChIP-seq	[20]	GSE167887

Deleted: s

Deleted: ¶

Page Break

References

1. Yesbolatova, A. *et al.* The auxin-inducible degron 2 technology provides sharp degradation control in yeast, mammalian cells, and mice. *Nat Commun* **11**, 5701 (2020).

2. Emerson, D. J. *et al.* Cohesin-mediated loop anchors confine the locations of human replication origins. *Nature* **606**, 812–819 (2022).

3. Yesbolatova, A., Natsume, T., Hayashi, K. & Kanemaki, M. T. Generation of conditional auxin-inducible degron (AID) cells and tight control of degron-fused proteins using the degradation inhibitor auxinole. *Methods* **164**, 73–80 (2019).

4. Ran, F. A. *et al.* Genome engineering using the CRISPR-Cas9 system. *Nat Protoc* **8**, 2281–2308 (2013).

5. Sirbu, B. M. *et al.* Analysis of protein dynamics at active, stalled, and collapsed replication forks. *Gene Dev* **25**, 1320–1327 (2011).

6. Sirbu, B. M., Couch, F. B. & Cortez, D. Monitoring the spatiotemporal dynamics of proteins at replication forks and in assembled chromatin using isolation of proteins on nascent DNA. *Nat Protoc* **7**, 594–605 (2012).

7. Quinet, A. *et al.* PRIMPOL-Mediated Adaptive Response Suppresses Replication Fork Reversal in BRCA-Deficient Cells. *Mol Cell* **77**, 461-474.e9 (2020).

8. Zellweger, R. & Lopes, M. Dynamic Architecture of Eukaryotic DNA Replication Forks In Vivo, Visualized by Electron Microscopy. *Methods Mol Biology Clifton N J* **1672**, 261–294 (2018).

9. Schindelin, J. *et al.* Fiji: an open-source platform for biological-image analysis. *Nat. Methods* **9**, 676–682 (2012).

10. Li, H. Aligning sequence reads, clone sequences and assembly contigs with BWA-MEM. *arXiv* (2013) doi:10.48550/arxiv.1303.3997.

11. Crane, E. *et al.* Condensin-driven remodelling of X chromosome topology during dosage compensation. *Nature* **523**, 240–244 (2015).

12. Matthey-Doret, C. *et al.* Computer vision for pattern detection in chromosome contact maps. *Nat. Commun.* **11**, 5795 (2020).

13. Liu, Y. *et al.* Fork coupling directs DNA replication elongation and termination. *Science* **383**, 1215–1222 (2024).

14. Flyamer, I. M., Illingworth, R. S. & Bickmore, W. A. Coolpup.py: versatile pile-up analysis of Hi-C data. *Bioinformatics* **36**, 2980–2985 (2020).

15. Koyanagi, E. *et al.* Global landscape of replicative DNA polymerase usage in the human genome. *Nat. Commun.* **13**, 7221 (2022).

16. Alonso-Gil, D., Cuadrado, A., Giménez-Llorente, D., Rodríguez-Corsino, M. & Losada, A. Different NIPBL requirements of cohesin-STAG1 and cohesin-STAG2. *Nat. Commun.* **14**, 1326 (2023).

17. Remeseiro, S. *et al.* Cohesin-SA1 deficiency drives aneuploidy and tumourigenesis in mice due to impaired replication of telomeres. *EMBO J.* **31**, 2076–2089 (2012).

18. González-Acosta, D. *et al.* PrimPol-mediated repriming facilitates replication traverse of DNA interstrand crosslinks. *Embo J* **40**, e106355 (2021).

19. Rao, S. S. P. *et al.* Cohesin Loss Eliminates All Loop Domains. *Cell* **171**, 305-320.e24 (2017).

20. Porter, H. *et al.* Cohesin-independent STAG proteins interact with RNA and R-loops and promote complex loading. *eLife* **12**, e79386 (2023).